

Nucleon electromagnetic form factors from scattering of polarized muons or electrons

B. M. Freedom

Department of Physics and Astronomy, University of South Carolina, Columbia, South Carolina 29208

R. Tegen*

*Department of Physics and Astronomy, University of South Carolina, Columbia, South Carolina 29208
and Institute of Theoretical Physics and Astrophysics, University of Cape Town, Rondebosch 7700, Republic of South Africa
(Received 20 May 1987)*

We investigate a new method of extracting nucleon form factors by using measured asymmetries of polarized leptons scattered off polarized targets. Systematic errors can be eliminated that way, unlike the conventional analysis via Rosenbluth plots. The kinematics can be chosen such that the asymmetry receives contributions selectively from either $G_M^2(q^2)$ or $G_E(q^2)G_M(q^2)$. The latter combination allows a better determination of $G_M(q^2)$ for small q^2 . We also discuss lepton mass effects in $d\sigma/d\Omega$. While such mass effects reduce the suppression of magnetic contributions to $d\sigma/d\Omega$ for small q^2 , they do not in general result in a greater sensitivity of $d\sigma/d\Omega$ or of the longitudinal asymmetries to a variation of the magnetic form factor, unless one chooses specific kinematics, as is demonstrated here. The transverse asymmetry, however, displays naturally a greater sensitivity to $G_M(q^2)$ for the muon as compared to the electron. Such experiments are feasible at both the electron facilities (Bates, CEBAF, MAMI, and ELSA) and the muon facilities (SIN, TRIUMF, and LAMPF). Constituent models of the nucleon (quark confinement models) emphasize the low $-q^2$ region of the form factors, where data presently are still incomplete. This has implications for the study of the nuclear response function in quasifree scattering ($\mu, \mu'p$) from nuclei using polarized muons.

I. INTRODUCTION

Recently nucleon form factors have regained much interest, both theoretical and experimental. Proposals for future electron scattering facilities [Bates,¹ CEBAF (Ref. 2)] have emphasized the study of the neutron charge form factor $G_E^n(q^2)$. In all of these experiments the lepton beam is an electron beam. At the meson factories, however, the pion beams produce a polarized muon (μ) beam which—as we will demonstrate below—can be used to remove persistent uncertainties in our knowledge of nucleon form factors.

The size of the nucleon [measured by the slope of the charge form factor $G_E(q^2)$ near zero] is ~ 0.85 fm, known only with a large uncertainty^{3,4} compared to other observables like its mass and magnetic moment. The corresponding neutron charge form factor is poorly known away from the rather precise thermal neutron on atomic electron scattering data [at very low four-momentum transfer squared $-q^2$ (Ref. 5)]. The magnetic form factors $G_M^{p,n}(q^2)$ are poorly known for very low q^2 (due to a kinematical suppression $\sim q^4$ for a nearly massless lepton beam) where the charge form factor $G_E(q^2)$ dominates [at high q^2 , $G_M(q^2)$ dominates the cross section]. Since the deviation of the magnetic form factor $G_M(q^2)$ from its value at $q^2=0$ describes both the charge and spin distribution inside the nucleon, the corresponding magnetic rms radius as compared to the charge rms radius is of interest for the understanding of the microscopic spin structure of the nucleon. Neither sign of $G_E(q^2)$ nor $G_M(q^2)$ can be determined by using

the standard technique of analysis via Rosenbluth plots.^{3,4}

The standard dipole fit for $G_E^p(q^2)$ and $G_M^p(q^2)$ provides an impressive overall description for $0 \leq -q^2 \leq 10$ (GeV/c)². However, the deviations from this purely phenomenological fit show up for both small and very high q^2 .^{4,6} The proton rms charge radius obtained from the dipole fit is $\langle r^2 \rangle^{1/2} = 0.81$ fm, whereas the data prefer a somewhat larger radius for the proton; furthermore, the dipole fit does not describe data well around

$$-q^2 \approx (0.3 - 0.4) (\text{GeV}/c)^2.$$

For the modeling of the hadrons in terms of their constituents (quarks and gluons) it is important to understand experimentally the charge form factor $G_E^p(q^2)$ in this region. It has been demonstrated that in chiral quark models the region $-q^2 \approx 0.3$ (GeV/c)² is the transition from probing the nucleon as a quasiparticle (a quark core with a surrounding pion cloud) to probing just the quark core.⁷ Beyond $-q^2 \approx 0.4$ (GeV/c)² the lepton beam does not probe the pion cloud any more. This is the region where perturbative quantum chromodynamics (QCD) starts to become applicable and the power law behavior $1/q^4$ for $G_{E,M}(q^2)$ emerges⁶ (without, however, explaining the magic number $1/\sqrt{2}$ GeV²/c² in the dipole fit).

We will show that using a muon instead of an electron beam has two advantages: (i) a highly polarized μ beam (both longitudinal and transverse polarization are possible) allows measuring the asymmetry for scattering from a polarized target, and (ii) one circumvents the kinemati-

cal q^4 suppression of the magnetic form factor $G_M^p(q^2)$ contribution to the cross section for small $-q^2$; this is a distinctive feature of the *muon* due to its non-negligible rest mass.

In the following we present the differential cross section for the scattering of massive, polarized leptons from polarized protons; this is a generalization of the well-known Rosenbluth formula.⁴ The most general case where *all* polarizations of leptons *and* protons are observed will not be considered here (see, for example, Ref. 8). We will sum over the spin polarization of the *outgoing* lepton and proton; this is presently the only feasible experimental situation.

II. NUCLEON ELECTROMAGNETIC FORM FACTORS

Given the conserved nucleon current $J_\mu(x)$, the relevant form factors are written in the form

$$\langle N(p', S') | J_\mu(0) | N(p, S) \rangle = \bar{u}(p', S') \left[F_1(q^2) \gamma_\mu + \frac{F_2(q^2)}{2M} i \sigma_{\mu\nu} q^\nu \right] u(p, S), \quad (1)$$

$$L_{\mu\nu} = \text{Tr} \left\{ \frac{\not{p}' + M}{2M} \left[\gamma_\mu G_M(q^2) - \frac{G_M(q^2) - G_E(q^2)}{2M(1+\eta)} (p' + p)_\mu \right] \times \frac{\not{p} + M}{2M} \frac{1 + \gamma_5 \not{s}}{2} \left[\gamma_\nu G_M(q^2) - \frac{G_M(q^2) - G_E(q^2)}{2M(1+\eta)} (p' + p)_\nu \right] \right\},$$

where m is the lepton mass, $s = (\lambda/m)(|\mathbf{k}|, \hat{\mathbf{E}}\hat{\mathbf{k}})$ and $\lambda \equiv \hat{\mathbf{k}} \cdot \hat{\mathbf{s}} = \pm 1$ for longitudinal polarization, and $s = (0, \hat{\mathbf{n}})$ with $\hat{\mathbf{k}} \cdot \hat{\mathbf{n}} = 0$ for transverse polarization, with $\hat{\mathbf{k}} = \mathbf{k}/|\mathbf{k}|$. In the rest system of the incoming proton we have $S' = (0, \hat{\mathbf{S}})$ and $p = (M, \mathbf{0})$. In the calculations presented below, a Cartesian coordinate system is chosen such that $\hat{\mathbf{z}} = \hat{\mathbf{k}}$, $\hat{\mathbf{y}} = \hat{\mathbf{k}} \times \hat{\mathbf{k}}'$, and $\hat{\mathbf{x}} = \hat{\mathbf{y}} \times \hat{\mathbf{z}}$.

A. Differential cross sections

After standard manipulations we obtain the differential cross section for the scattering of massive leptons from protons,¹⁰

$$\frac{d\sigma}{d\Omega} = \left[\frac{d\sigma}{d\Omega} \right]^{ns} R,$$

where

$$\left[\frac{d\sigma}{d\Omega} \right]^{ns} = \frac{\alpha^2}{4E^2} \frac{1 - \frac{-q^2}{4EE'}}{\left[\frac{-q^2}{4EE'} \right]^2} \times \frac{1/d}{\left[1 + \frac{2Ed}{M} \sin^2 \frac{\theta}{2} + \frac{E}{M} (1-d) \right]} \quad (2)$$

where $u(p, S)$ are the nucleon spinors, p and p' are ingoing and outgoing nucleon four-momenta with $p^2 = p'^2 = M^2$, the square of the nucleon mass, S and S' are the corresponding polarization four-vectors, and $q_\mu = (p' - p)_\mu$ is the four-momentum transfer. It is convenient to introduce the Sachs form factors,

$$G_E(q^2) = F_1(q^2) - \eta F_2(q^2), \quad G_M(q^2) = F_1(q^2) + F_2(q^2),$$

where $\eta = -q^2/4M^2 \geq 0$. Since the derivation of the Rosenbluth formula is standard, we indicate only where the polarization and lepton mass enter. To lowest order in the fine structure constant α , knowing the polarization of the incoming lepton beam alone does not produce any asymmetry.⁹ We consider therefore both a polarized lepton beam *and* a polarized target (proton). Let $k = (E, \mathbf{k})$ and $k' = (E', \mathbf{k}')$ be the four-momenta of the incoming and outgoing leptons; s and s' are the corresponding polarization four-vectors. The lepton and hadron tensors are

$$l^{\mu\nu} = \text{Tr} \left[\frac{\not{k}' + m}{2m} \gamma^\mu \frac{\not{k} + m}{2m} \frac{1 + \gamma_5 \not{s}'}{2} \gamma^\nu \right],$$

and

is the "no structure" cross section, with

$$d \equiv \left[\left[1 - \frac{m^2}{E^2} \right] / \left[1 - \frac{m^2}{E'^2} \right] \right]^{1/2}$$

and θ is the scattering angle between \mathbf{k} and \mathbf{k}' , and

$$q^2 = -4EE' \sin^2 \frac{\theta}{2} \left[\left[1 - \frac{m^2}{E^2} \right] \left[1 - \frac{m^2}{E'^2} \right] \right]^{1/2} + 2m^2 - 2EE' \left\{ 1 - \left[\left[1 - \frac{m^2}{E^2} \right] \left[1 - \frac{m^2}{E'^2} \right] \right]^{1/2} \right\}, \quad (3)$$

and

$$R = \frac{G_E^2(q^2) + \eta G_M^2(q^2)}{1 + \eta} + \left[2\eta - \frac{m^2}{M^2} \right] G_M^2(q^2) \frac{\frac{-q^2}{4EE'}}{\left[1 - \frac{-q^2}{4EE'} \right]}. \quad (4)$$

For $m=0$ we have $-q^2/4EE' = \sin^2(\theta/2)$, $d \equiv 1$, and $(d\sigma/d\Omega)^{ns} R$ reduces to the well-known Rosenbluth formula.⁴ For $m=0$ the θ dependent term (for fixed q^2) $2\eta G_M(q^2) \tan^2(\theta/2)$ serves to disentangle $G_E(q^2)$ and

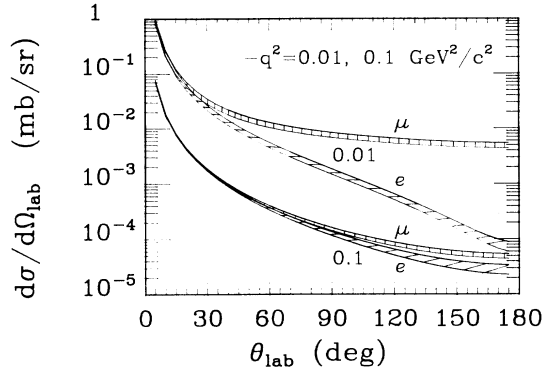


FIG. 1. Cross sections calculated from Eq. (2) as a function of laboratory angle, for $-q^2=0.01$ and 0.1 (GeV/c) 2 . The bands (horizontal lines for the electron; vertical lines for the muon) show the effect of a $\pm 10\%$ change in the magnitude of $G_M(q^2)$. The lower boundary corresponds to the 10% reduced $G_M(q^2)$.

$G_M(q^2)$. This term is very small in the interesting region of small q^2 , leading to large errors for $G_M(q^2)$ close to $q^2=0$.⁴ According to our Eq. (4) a muon beam would lead to much less suppression of the G_M^2 term for small $-q^2$, due to $(2\eta - m^2/M^2)$ instead of 2η . For a muon $(m_\mu/M)^2=0.0127$ is non-negligible, whereas for the electron $(m_e/M)^2 \approx 3 \times 10^{-7}$ is totally negligible. Thus the magnetic form factor for small $-q^2 \approx 0$ could in principle be better determined with a muon beam. Cross sections calculated from Eq. (2) are shown as a function of laboratory scattering angle for different q^2 in Fig. 1. The muon cross section is always higher than that of the electron, reflecting the fact that, for the same momentum transfer, the muon has a lower kinetic energy. All of the calculations shown in the figures use the dipole form factor for the proton, where

$$G_E(q^2) = \left[1 + \frac{-q^2}{0.71 \text{ GeV}^2/c^2} \right]^{-2},$$

and the isoscaling law⁴

$$\begin{aligned} \mathbf{A}_{\parallel} = & \frac{1}{(1+\eta) \left[1 - \frac{-q^2}{4EE'} \right]} \left\{ \eta G_M^2(q^2) \left[\hat{\mathbf{k}} \left[\frac{E^2 - m^2}{2ME} - \frac{E^2 - m^2}{EE'} - \frac{|\mathbf{k}| |\mathbf{k}'|}{2ME'} \cos\theta \right] \right. \right. \\ & \left. \left. + \hat{\mathbf{k}}' \left[\frac{E'^2 - m^2}{2ME'} \cos\theta + \frac{|\mathbf{k}| |\mathbf{k}'|}{EE'} \left[1 - \frac{E'}{2M} \right] \right] \right\} \\ & + G_E(q^2) G_M(q^2) \left\{ \hat{\mathbf{k}} \left[\frac{E^2 - m^2}{2ME'} - \frac{|\mathbf{k}| |\mathbf{k}'|}{2ME'} \cos\theta - \frac{2M}{E'} \eta (1+\eta) \right] \right. \\ & \left. \left. + \hat{\mathbf{k}}' \left[\frac{E'^2 - m^2}{2ME'} \cos\theta - \frac{|\mathbf{k}| |\mathbf{k}'|}{2ME'} \right] \right\} \right\} \end{aligned} \quad (5b)$$

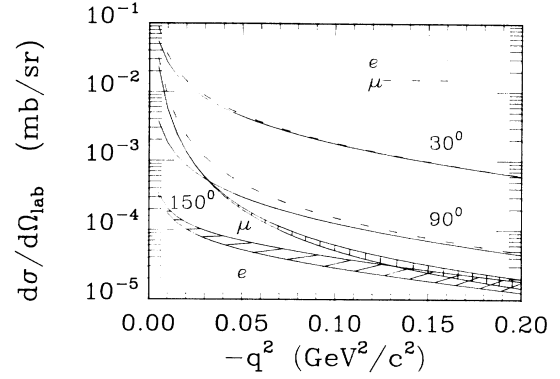


FIG. 2. Cross sections as a function of $-q^2$ for different scattering angles $\theta_{\text{lab}}=30^\circ, 90^\circ,$ and 150° . The bands show the effect of a $\pm 10\%$ change in $G_M(q^2)$; otherwise as in Fig. 1.

$$G_M(q^2) = 2.79 G_E(q^2).$$

Figure 1 also shows the effect of a $\pm 10\%$ change in the magnitude of $G_M(q^2)$ for $-q^2=0.01$ and 0.1 (GeV/c) 2 . The effect for such a change in $G_E(q^2)$ is generally larger (not shown here).

In Fig. 2 the cross sections are shown as a function of $-q^2$ for different scattering angles $\theta=30^\circ, 90^\circ,$ and 150° . The muon cross section is larger than the electron cross section and displays roughly the same sensitivity as the electron to the variation of $G_E(q^2)$ (not shown here). The variation of $G_M(q^2)$ is shown here only for $\theta=150^\circ$; at smaller angles the variation shows a much smaller effect. From this variation it is seen that the electron cross section is more sensitive than the muon cross section, in particular for low $-q^2$.

B. Longitudinal polarization ($\lambda=\pm 1$)

$$\frac{d\sigma}{d\Omega} = \left[\frac{d\sigma}{d\Omega} \right]^{ns} (R + \lambda \hat{\mathbf{S}} \cdot \mathbf{A}_{\parallel}), \quad (5a)$$

where

Note that $(\hat{\mathbf{S}} \cdot \mathbf{A}_{\parallel})$ vanishes identically for $\hat{\mathbf{S}}$ perpendicular to the scattering plane, independent of the lepton mass. Also note that the vector multiplying G_M^2 is orthogonal to that multiplying $G_E G_M$. Thus the two terms can be easily separated by choosing a suitable target polarization. The asymmetry due to the presence of \mathbf{A}_{\parallel} , in Eq. (5a) has been discussed in the limit $m=0$ in the literature.¹¹

Let P be the polarization degree of the lepton beam, i.e., $P = P_R - P_L$; then the asymmetry is given by

$$A_{\parallel} = P \frac{d\sigma(\lambda = +1, \hat{\mathbf{S}}) - d\sigma(\lambda = +1, -\hat{\mathbf{S}})}{d\sigma(\lambda = +1, \hat{\mathbf{S}}) + d\sigma(\lambda = +1, -\hat{\mathbf{S}})}; \quad (6)$$

and it is determined by \mathbf{A}_{\parallel} , Eq. (5). Of course the same equation obtains for a constant target polarization with λ changing from $+1$ to -1 .¹² The asymmetry is sensitive to the sign of $G_E G_M$,¹³ whereas the Rosenbluth formula R of Eq. (4) does not allow one to determine the sign of G_E or G_M . It is indeed possible to choose the orientation of the target polarization such that *only* the $G_E G_M$ term in \mathbf{A}_{\parallel} , Eq. (5b), contributes to the asymmetry. For $m=0$ this is achieved for a specific orientation of the polarization $\hat{\mathbf{S}}$ relative to the lepton momenta \mathbf{k}, \mathbf{k}' , namely

$$\hat{\mathbf{k}} \cdot \hat{\mathbf{S}} = \hat{\mathbf{k}}' \cdot \hat{\mathbf{S}} \frac{E'}{E} = \left(\frac{E'}{E} \right)^{1/2} \cos \frac{\theta}{2} \frac{1}{\sqrt{1+\eta}}, \quad (7)$$

or, equivalently, $\mathbf{q} \cdot \hat{\mathbf{S}} = 0$, i.e., the target polarization is perpendicular to the photon three-momentum \mathbf{q} . In this case ($m=0$) we find

$$(1+\eta)\hat{\mathbf{S}} \cdot \mathbf{A}_{\parallel} = -2\sqrt{\eta(1+\eta)} \tan \frac{\theta}{2} G_E(q^2) G_M(q^2). \quad (8)$$

For $m \neq 0$, the $G_E G_M$ term can be selected in the asymmetry by requiring that

$$\hat{\mathbf{k}} \cdot \hat{\mathbf{S}} = \hat{\mathbf{k}}' \cdot \hat{\mathbf{S}} \frac{E'}{E} \frac{\frac{E'}{M} \sin^2 \frac{\theta}{2} - 1 - \frac{m^2}{M^2} a_1}{\frac{E'}{M} \sin^2 \frac{\theta}{2} - 1 - \frac{m^2}{M^2} b_1}, \quad (9)$$

with

$$\frac{a_1}{M^2} \equiv \frac{\cos \theta}{2ME'} - \left[1 + \frac{E'}{2M} \right] \frac{\Delta}{m^2},$$

$$\frac{b_1}{M^2} \equiv \frac{E' - 2M}{2ME^2} - \frac{E' \cos \theta}{2M} \frac{\Delta}{m^2},$$

and

$$\begin{aligned} \Delta &\equiv 1 - \left[\left[1 - \frac{m^2}{E^2} \right] \left[1 - \frac{m^2}{E'^2} \right] \right]^{1/2} \\ &= \frac{m^2}{2} \left[\frac{1}{E^2} + \frac{1}{E'^2} \right] + O(m^4). \end{aligned}$$

Note that for $m \neq 0$ the condition $\mathbf{q} \cdot \hat{\mathbf{S}} = 0$ would imply [instead of Eq. (9)],

$$\begin{aligned} \hat{\mathbf{k}} \cdot \hat{\mathbf{S}} &= \hat{\mathbf{k}}' \cdot \hat{\mathbf{S}} \frac{k'}{k} \\ &= \cos \frac{\theta}{2} \left[\frac{k'}{k} \right]^{1/2} \frac{1}{\left[1 + (k - k')^2 / 4kk' \sin^2 \frac{\theta}{2} \right]^{1/2}}, \end{aligned}$$

where $k = |\mathbf{k}|$, $k' = |\mathbf{k}'|$.

Similarly, it is possible to arrange beam orientation and target polarization such that the $G_E G_M$ term in \mathbf{A}_{\parallel} , Eq. (5), vanishes and only the G_M^2 term determines the asymmetry. For the case of $m=0$, this can be achieved for

$$\hat{\mathbf{k}} \cdot \hat{\mathbf{S}} = \hat{\mathbf{k}}' \cdot \hat{\mathbf{S}} \frac{1 + \frac{M}{E}}{1 - \frac{M}{E'}} = \sin \frac{\theta}{2} \frac{E + M}{M} \left[\frac{E'}{E} \right]^{1/2} \frac{1}{\sqrt{1+\eta}}$$

or, equivalently, $\mathbf{q} \cdot \hat{\mathbf{S}} = |\mathbf{q}|$, i.e., the target polarization must be parallel to the photon three-momentum. In this case ($m=0$)

$$(1+\eta)\hat{\mathbf{S}} \cdot \mathbf{A}_{\parallel} = -\frac{E + E'}{M} \sqrt{\eta(1+\eta)} \tan^2 \frac{\theta}{2} G_M^2(q^2).$$

For $m \neq 0$, the $G_E G_M$ term vanishes if

$$\hat{\mathbf{k}} \cdot \hat{\mathbf{S}} = \hat{\mathbf{k}}' \cdot \hat{\mathbf{S}} \frac{1 + \frac{M}{E} - \frac{m^2}{M^2} a_3}{1 - \frac{M}{E'} - \frac{m^2}{M^2} b_3}, \quad (10)$$

with

$$\frac{a_3}{M^2} \equiv \frac{E' - M \cos \theta + (M - E' \cos \theta) E E' \frac{\Delta}{m^2}}{2E E'^2 \sin^2 \frac{\theta}{2}},$$

$$\frac{b_3}{M^2} \equiv \frac{(E' - M) \left[1 - E E' \cos \theta \frac{\Delta}{m^2} \right]}{2E E'^2 \sin^2 \frac{\theta}{2}}.$$

Note that $\mathbf{q} \cdot \hat{\mathbf{S}} = |\mathbf{q}|$ in this case ($m \neq 0$) would imply [instead of Eq. (10)]

$$\begin{aligned} \hat{\mathbf{k}} \cdot \hat{\mathbf{S}} &= \hat{\mathbf{k}}' \cdot \hat{\mathbf{S}} \frac{k - k' \cos \theta}{k \cos \theta - k'} \\ &= \sin \frac{\theta}{2} \left[\frac{k'}{k} \right]^{1/2} \frac{1 + \frac{k - k'}{2k' \sin^2 \frac{\theta}{2}}}{\left[1 + (k - k')^2 / 4kk' \sin^2 \frac{\theta}{2} \right]^{1/2}}, \end{aligned}$$

where again $k = |\mathbf{k}|$ and $k' = |\mathbf{k}'|$. For $m \neq 0$ the kinematics have to be chosen such that Eq. (10) holds; then the asymmetry is only sensitive to $G_M^2(q^2)$.

C. Transverse polarization ($\hat{\mathbf{k}} \cdot \hat{\mathbf{n}} = 0$)

$$\frac{d\sigma}{d\Omega} = \left[\frac{d\sigma}{d\Omega} \right]^{ns} (R + \hat{\mathbf{S}} \cdot \mathbf{A}_{\perp}), \quad (11)$$

where

$$\mathbf{A}_\perp = \frac{-\frac{m}{M}}{(1+\eta) \left[1 - \frac{-q^2}{4EE'} \right]} \frac{1}{2EE'} \times \{ \eta G_M^2(q^2) \mathbf{q}(\mathbf{k}' \cdot \hat{\mathbf{n}}) + G_E(q^2) G_M(q^2) [4M^2 \eta (1+\eta) \hat{\mathbf{n}} + \mathbf{q}(\mathbf{k}' \cdot \hat{\mathbf{n}})] \} . \quad (12)$$

Note that $\mathbf{A}_\perp \sim m$ vanishes for $m \rightarrow 0$, as expected. Since \mathbf{A}_\perp has a component $\sim \hat{\mathbf{n}}$ it does *not* vanish for $\hat{\mathbf{S}}$ perpendicular to the scattering plane.

For *transverse* lepton polarization the G_M^2 term in Eq. (12) vanishes if either $\hat{\mathbf{k}}' \cdot \hat{\mathbf{n}} = 0$ or $\hat{\mathbf{S}} \cdot \mathbf{q} = 0$. This can be achieved for $\hat{\mathbf{S}} \cdot \hat{\mathbf{k}} = \hat{\mathbf{S}} \cdot \hat{\mathbf{k}}' = 0$ and $\hat{\mathbf{S}} \cdot \hat{\mathbf{n}} \neq 0$, i.e., for target polarization perpendicular to the scattering plane. In this case a nonzero lepton mass m will give a contribution to the asymmetry

$$\hat{\mathbf{S}} \cdot \mathbf{A}_\perp = -\frac{mM}{EE'} 2\eta \left[\frac{\hat{\mathbf{S}} \cdot \hat{\mathbf{n}}}{1 - \frac{-q^2}{4EE'}} \right] G_E(q^2) G_M(q^2) .$$

III. DISCUSSION

Calculations were made for various polarization configurations using the equations presented in Secs. II B and II C above. The asymmetry calculations presented below assume beam polarizations and target polarizations of 100%.

Two examples for longitudinal asymmetries for electrons and muons are presented in Fig. 3. In Figs. 3(a) and 3(b) the target polarization is such that only the G_M^2 term of Eq. (5) exists. For this specific kinematics the muon asymmetry is more sensitive than the electron asymmetry to both G_E (not shown) and G_M for $\theta \gtrsim 50^\circ$. In all other cases the electron asymmetry is more sensitive than the muon asymmetry to both G_E and G_M . Longitudinal asymmetries for target polarization in the z direction (i.e., along the beam direction) are very similar to the curves shown in Figs. 3(a) and 3(b) (although, generally, they have slightly more negative asymmetries). In Figs. 3(c) and 3(d) the target polarization is chosen such that only the $G_E G_M$ term of Eq. (5) exists. The general shape of the curves changes with a minimum between $\theta_{\text{lab}} = 100^\circ$ and 150° , and a vanishing asymmetry at the backward angle $\theta = 180^\circ$ [see Fig. 3(c)]. The electron displays significantly more asymmetry than the muon at low ($-q^2$), with the larger asymmetry occurring at large angles. In each case the electron asymmetry is more sensitive than the muon asymmetry to both G_E (not shown) and G_M at large angles [see Figs. 3(c) and 3(d)]. Longitudinal asymmetries for target polarizations in the x direction are very similar to the curves shown in Figs. 3(c) and 3(d) (although, generally with less negative asymmetries).

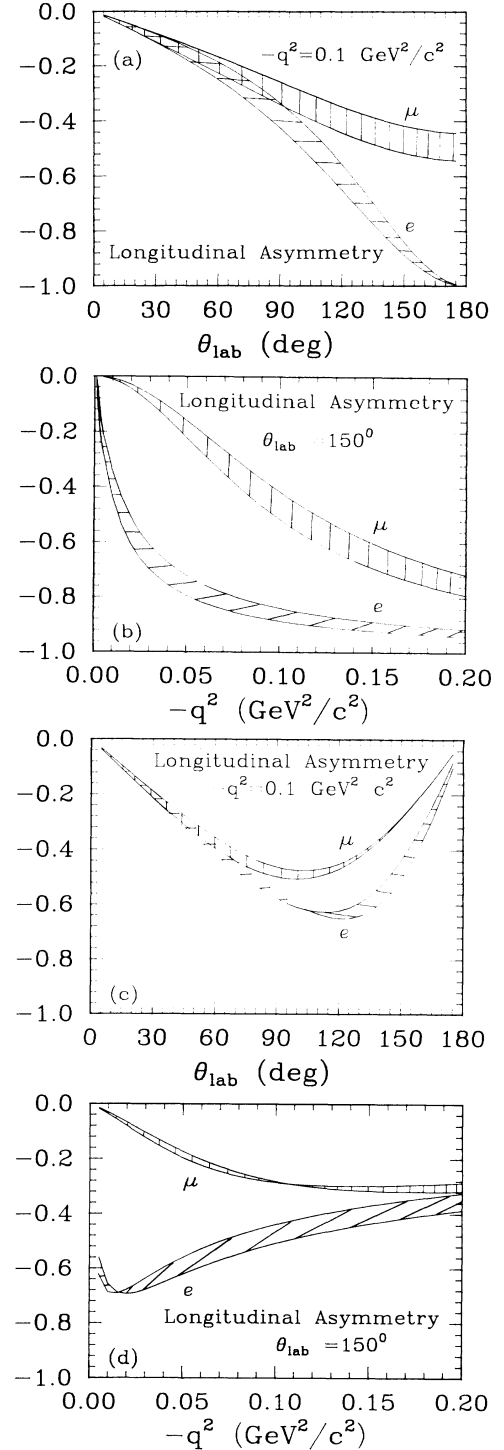


FIG. 3. (a) Longitudinal asymmetry as a function of θ_{lab} , for $-q^2 = 0.1 \text{ (GeV/c)}^2$. Target polarization and beam axis are oriented such that the $G_E G_M$ term in Eq. (5) vanishes identically; see text. The beam is assumed to be 100% polarized. The bands correspond to a 10% variation of $G_M(q^2)$, with the upper boundary corresponding to the 10% reduced $G_M(q^2)$ in the cross section. (b) Longitudinal asymmetry as a function of $-q^2$, for $\theta_{\text{lab}} = 150^\circ$; otherwise as in (a). (c), (d) Target polarization and beam axis are oriented such that the G_M^2 term in Eq. (5) vanishes; otherwise as in (a), (b).

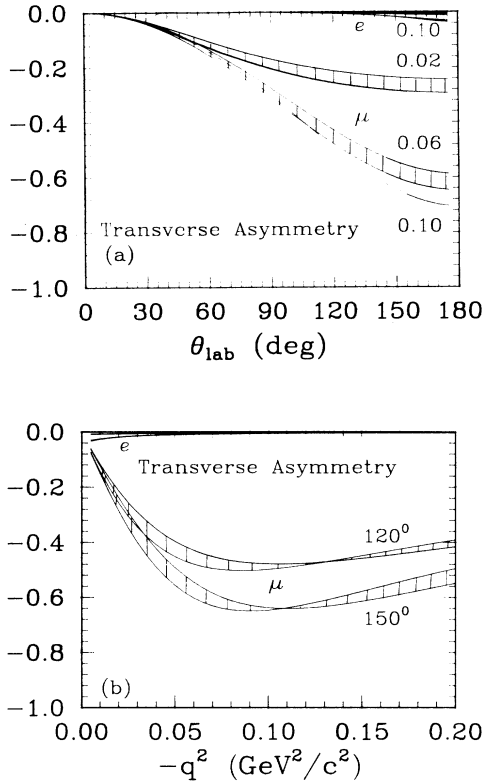


FIG. 4. (a) Transverse asymmetry as a function of θ_{lab} for $-q^2 = 0.02, 0.06,$ and 0.1 $(\text{GeV}/c)^2$. The target polarization is perpendicular to the scattering plane. Otherwise as in Fig. 3(a). (b) As in (a) but now as a function of $-q^2$ for $\theta_{\text{lab}} = 120^\circ$ and 150° . For $-q^2 \leq 0.10$ $(\text{GeV}/c)^2$ the upper boundary of the bands corresponds to the 10% reduced $G_M(q^2)$ in $d\sigma/d\Omega$. In the region of $-q^2 = 0.10$ to 0.15 $(\text{GeV}/c)^2$ there is a crossover in the $\pm 10\%$ curves; see text.

Transverse asymmetries are shown in Fig. 4. In these calculations, the lepton polarization and the target polarization are in the y direction (i.e., out of the scattering plane). The electron asymmetry is essentially zero because of its small rest mass. In Fig. 4(a), the transverse asymmetry is displayed as a function of scattering angle for $-q^2 = 0.02$ and 0.06 $(\text{GeV}/c)^2$. Also shown are calculations with G_M changed by $\pm 10\%$ (results with G_E changed by $\pm 10\%$ are very similar and are, therefore, not shown here). There are significant changes at large angles except for $-q^2 = 0.1$ $(\text{GeV}/c)^2$. The reason for this can be seen in Fig. 4(b) where the transverse asymmetry is shown as a function of q^2 for scattering angles of 120° and 150° . In the region of 0.10 to 0.15 $(\text{GeV}/c)^2$,

there is a crossover in the $\pm 10\%$ curves indicating that such a change in G_M results in a change of the shape of the q^2 dependence.

IV. CONCLUSION

We propose a new method of extracting nucleon form factors by using measured asymmetries of polarized leptons. Such asymmetries turn out to be sizable, and they arise from differences in the differential cross sections $d\sigma/d\Omega$ for polarized lepton scattering from a polarized target. Expected differential cross sections for the energy range $E \gtrsim 200$ MeV are measurable [$\gtrsim 1/10$ $\mu\text{b}/\text{sr}$ for $-q^2 \lesssim 0.1$ $(\text{GeV}/c)^2$ at backward angles] at existing facilities. Systematic errors can be eliminated to a large extent in the asymmetries, which is not so easy for the conventional analysis via Rosenbluth plots. Moreover, the kinematics can be chosen such that the asymmetry receives contributions selectively from either $G_M^2(q^2)$ or $G_E(q^2)G_M(q^2)$. The latter combination allows a better determination of $G_M(q^2)$ for small q^2 . We have also discussed lepton mass effects in $d\sigma/d\Omega$. While such mass effects reduce the suppression of magnetic contributions to $d\sigma/d\Omega$ for small q^2 , they do not in general result in a greater sensitivity of $d\sigma/d\Omega$ or of the longitudinal asymmetries to a variation of the magnetic form factor [unless one chooses specific kinematics as in Figs. 3(a) and 3(b)]. The transverse asymmetry, however, displays naturally a greater sensitivity to $G_M(q^2)$ for the muon as compared to the electron. Such experiments are feasible at both the electron facilities (Bates, CEBAF, MAMI, ELSA) and the muon facilities (SIN, TRIUMF, and LAMPF). Such experiments with muon beams also provide another test of the μ - e universality hypothesis. Constituent models of the nucleon (quark confinement models) emphasize the low- q^2 region of the form factors, where data presently are still incomplete. Finally, we note an extension of these ideas to quasifree scattering ($\mu, \mu'p$) from nuclei using polarized muons. Without using polarized targets one can compare the transverse and longitudinal components by measuring $\mu'p$ correlations out of the μ' -beam plane and thus study a nuclear response function unavailable to electrons.

ACKNOWLEDGMENTS

The authors would like to acknowledge useful discussions with L. M. Simons, H. G. Andresen, and E. Moniz. We would like to thank Fred Myhrer for his careful reading of the manuscript. This work was supported in part by a grant from the U.S. National Science Foundation (B.M.P.) and from the South African Council for Scientific and Industrial Research—Foundation for Research Development (R.T.).

*Permanent address: Institute of Theoretical Physics and Astrophysics, University of Cape Town, Rondebosch 7700, Republic of South Africa.

¹Report of the Workshop on Future Directions in Electromagnetic Nuclear Physics, Part 2, 1980, Massachusetts Institute

of Technology Report (unpublished); T. W. Donnelly, in Proceedings of the Third Workshop of the Bates Users Theory Group, Massachusetts Institute of Technology, 1984, edited by G. Rawitscher (unpublished).

²CEBAF, 1986, CEBAF Design Report (unpublished); F.

- Gross in Proceedings of the CEBAF/SURA 1986 Summer Workshop, CEBAF, Newport News, Virginia, 1986, edited by F. Gross and R. Minehart (unpublished).
- ³F. Borkowski *et al.*, *Z. Phys. A* **275**, 29 (1975), *Nucl. Phys. B* **93**, 461 (1975).
- ⁴G. Höhler, *Pion Nucleon Scattering*, in Group I, Vol. 9, Subvol. b, Pt. 2 of Landolt-Börnstein, New Series, *Numerical Data and Functional Relationships in Science and Technology*, edited by H. Schopper, Springer-Verlag, Heidelberg, 1983) Chap. 2.5; M. Gourdin, *Phys. Rep.* **11C**, 29 (1974); M. N. Rosenbluth, *Phys. Rev.* **79**, 615 (1950).
- ⁵V. E. Krohn *et al.*, *Phys. Rev. D* **8**, 1305 (1973); L. Koester *et al.*, *Phys. Rev. Lett.* **36**, 1021 (1976).
- ⁶S. J. Brodsky and G. P. Lepage, *Phys. Scr.* **23**, 945 (1981); G. P. Lepage and S. J. Brodsky, *Phys. Rev. D* **22**, 2157 (1980). For a review see S. J. Brodsky, in *Quarks and Nuclear Forces*, Vol. 100 of *Springer Tracts in Modern Physics*, edited by D. C. Fries and B. Zeitnitz (Springer, New York, 1982), p. 81.
- ⁷R. Tegen, R. Brockmann and W. Weise, *Z. Phys. A* **307**, 339 (1982); E. Oset, R. Tegen and W. Weise, *Nucl. Phys.* **A426**, 456 (1984); S. Thèberge, G. A. Miller and A. W. Thomas, *Can. J. Phys.* **60**, 59 (1982); S. Thèberge and A. W. Thomas, *Nucl. Phys.* **A393**, 252 (1983).
- ⁸T. Garavaglia, *Int. J. Theor. Phys.* **23**, 251 (1984); *Nuovo Cimento* **56A**, 121 (1980).
- ⁹An asymmetry can come from the loop diagrams at the α' level, and at the order 10^{-5} can arise from the interference between the electromagnetic amplitude (associated with the exchange of one photon) and the parity violating weak amplitude (associated with the exchange of the Z^0 boson); see R. M. Cahn and F. J. Gilman, *Phys. Rev. D* **17**, 1313 (1978); V. W. Hughes, *High Energy Physics with Polarized Beams and Polarized Targets (Argonne, 1978)*, Proceedings of the Third International Symposium on High Energy Physics with Polarized Beams and Polarized Targets, AIP Conf. Proc. No. 51, edited by G. H. Thomas (AIP, New York, 1979), p. 171.
- ¹⁰Our Eq. (2) corresponds with Eq. (16) of S. D. Drell and J. D. Walecka, *Ann. Phys. (N.Y.)* **28**, 18 (1964).
- ¹¹N. Dombey, *Rev. Mod. Phys.* **41**, 236 (1969). M. Gourdin, Ref. 4.
- ¹²The target polarization can be easily reversed using modern laser technology. This technique has been redefined at Mainz University and will be extensively used for future polarization experiments at the Mainz Microtron (MAMI) facility (H. G. Andresen, private communication).
- ¹³The asymmetry in electron-proton elastic scattering has been used at SLAC to determine the sign of $G_E G_M$ to be positive at one kinematic point [$E=6.47$ GeV, $\theta=8^\circ$, and $-q^2=0.76$ (GeV/c) 2], M. J. Alguard *et al.*, *Phys. Rev. Lett.* **37**, 1258 (1976); see also Hughes, Ref. 9.